

SIMULATION OF PCCV WITH GROUTED OR NON-GROUTED TENDONS

Kim Calonius¹, Pekka Välikangas²

¹ Research Scientist, Structural Integrity Team, Technical Research Centre of Finland (VTT)
(kim.calonius@vtt.fi)

² Section Head, Civil Engineering and Fire Protection, Radiation and Nuclear Safety Authority (STUK),
Finland

ABSTRACT

There were two main goals in this study. The first one was to take in use a common calculation model that was presented for the round-robin benchmark SPE3 launched by OECD concerning the International Standard Problem ISP48 and use it to evaluate the ultimate failure capacity of a tested Prestressed Concrete Containment Vessel (PCCV) structure for which the calculation model was created. The second one was to compare methodologies for simulating bonded (cement grouted) tendons and unbonded (non-grouted, usually greased/waxed) tendons for post-tensioning of PCCV. This comparison was made mainly regarding the ultimate failure capacity of the test model against inner overpressure. It required two slightly different finite element (FE) models. These methodologies were also compared with each other by using the knowledge gathered during the OECD benchmark mentioned above.

The force distribution in the tendons before the overpressurisation was able to be modelled in a correct manner by simulating the pulling of tendons, anchor seating and locking. The simulated distribution was verified against simplified analytical calculation and some experimental measurements.

The FE model was capable of predicting the behaviour of the PCCV during the post-tensioning phase as well as in case of increasing overpressure up to the point of rupture. The FE model predicted the rupture pressure somewhat too high. The test model ruptured finally between the two main penetrations. The FE model suggests the corresponding location as very probable, but it is difficult to designate any single location.

The analyses in this study did not show any major differences between the results with bonded and unbonded methodologies at least not from basic design point of view. According to them, there was no essential difference between the ultimate capacities in these two cases. However, it seems that the model is not capable of simulating the tendon slipping and thus the redistribution of tendon stresses efficiently enough during overpressurisation. In some other computational studies, differences with these methods have been observed, but they have not been consistent studywise.

INTRODUCTION

As long as PCCVs have been designed, built and monitored there has been discussion on corresponding pros and cons between bonded and unbonded tendon solutions in post-tensioning. An important issue under discussion is the reliability of analysis methods and tools in order to verify design criteria and lifetime behavior of PCCV. This paper is concentrating on analysis methods and tools as well as feedback received when analysis results have been compared with testing results. Work behind the paper has been done with finance from Finnish radiation and nuclear safety authority (STUK). An important part of the results has been received from the international co-operation in the OECD NEA/CSNI launched activity "OECD Post Tensioning Methodologies for Containment Building: Greased or Cement Grouted Tendons - Consequences on Monitoring, Periodic Testing and Modelling Activities", where advantages and disadvantages of grouted and non-grouted technologies alongside one another have

been studied. This paper is concentrating on modelling part of the activity, and the modelling is focused on the beyond design accident overpressure.

The Nuclear Power Engineering Corporation (NUPEC) of Japan and the U.S. Nuclear Regulatory Commission (NRC), Office of Nuclear Regulatory Research, cosponsored and jointly funded a Cooperative Containment Research Program at Sandia National Laboratories (SNL) from July, 1991 till December, 2002. As part of this program, a 1:4 scale model of a PCCV was constructed and pressure-tested to failure. The prototype for the model is the containment building of Unit 3 of the Ohi Nuclear Power Station in Japan. The design accident overpressure, P_d , of both the prototype and the model is 0.39 MPa. It is referred to many times in this paper. The objectives of the test, also known as ISP48 (International Standard Problem), were to simulate some aspects of the severe accident loads on containment vessels, observe the model failure mechanisms, and obtain structural response data up to failure for comparison with analytical models.

The first goal of this study was to take in use a common calculation model that was presented for the round-robin benchmark SPE3 within the OECD activity mentioned above, to improve it further and to use it to simulate the Structural Failure Mode Test (SFMT) of ISP48. That alone involves many difficult questions concerning modern and novel simulation procedures. The second one was to compare the two post-tensioning methodologies with each other; the ones based on either bonded or unbonded tendons. This comparison is mainly based on the finite element (FE) simulations by the authors, but also other knowledge gathered from the OECD activities has been used.

DESCRIPTION OF ISP48 TEST

All the details of the ISP48 test are reported by Hessheimer et al. (2003) and by Dameron et al. (2003), but some main aspects are explained here. The main tests, the Limit State Test (LST) (terminated at $3.3 P_d$) and SFMT (total failure at $3.63 P_d$) were conducted in 2000 and 2002, respectively. The test containment was a thin prestressed concrete cylindrical shell with a hemispherical dome and a continuous steel liner anchored to a reinforced concrete basemat. In the test model, many local details, particularly the main penetrations and the areas around them, were represented. The liner and concrete reinforcing details around these penetrations were also retained. The photograph of the intact test model is shown in Figure 1. The outer diameter, height and main wall thickness of the cylinder were 11.4 m, 10.75 m and 0.325 m, respectively.

A 1.6 mm thick steel liner was applied to the inner surface of the concrete wall. The reinforcement consisted of longitudinal reinforcement bars (called rebars from hereon), transverse rebars and 188 tendons which run in hoop direction (once around and both ends anchored to the same buttress) and over the containment as a shape of an inverted U-letter (also called hairpin tendons). An unbonded prestressing system was used, where the tendons consisted of three seven-wire strands, each with a diameter of 13.7 mm. The tendons were inserted in galvanized metal sheath or ducts after the concrete had been placed and allowed to cure, then tensioned. The tensioning forces were locked in by seating the strands in the anchor blocks using tapered wedges. During this process, there was some loss of anchor force due to slipping and settling of the anchor components. The so-called seating loss, the shortening of the tendon during seating, was 5 mm.

The LST was designed to fulfill the primary objectives of the PCCV test program, i.e. to investigate the response of representative models of nuclear containment structures to pressure loading beyond the design basis accident and to compare analytical predictions to measured behaviour. It was conducted by slowly pressurizing the model using nitrogen gas. A leak, presumably through a tear in the liner, was first detected at a pressure of $2.5 P_d$. The liner strains in the vicinity of the equipment hatch (E/H; see Fig. 1), the largest opening, exceeded 1%. The test was terminated when the model reached a pressure of $3.3 P_d$ and the leak rate was exceeding the capacity of the pressurization system. Post-test inspections revealed 26 tears in the 1.6 mm thick steel liner as the source of the leaks. The largest crack was observed to the left of the E/H. Otherwise, there was no evidence of excessive structural damage or yielding.

Since only limited damage and inelastic response occurred during the LST, the interior was re-sealed with an elastomeric membrane. The PCCV was then filled nearly full with water and repressurised during SFMT. At approximately $3.3 P_d$, the acoustic system recorded a very high noise level event which was interpreted as the breaking of a tendon wire. After this point, events occurred very quickly. Shortly after detecting the wire break, a small spray of water was observed at approximately 0° azimuth, between E/H and A/L (representing personnel airlock), at global Y-direction in the calculation model, and additional tendon wire breaks were detected by the acoustic system with increasing frequency. SFMT reached a maximum pressure of $3.63 P_d$ when the model ruptured violently at approx. 6° azimuth near the mid-height of the cylinder by failure of the pre-stressing tendons and then the reinforcing steel. The maximum displacements were approx. 50 mm at the instant of final rupture and loss of pressure.

CONSIDERATIONS WITHIN OECD BENCHMARK

Grouted and non-grouted post-tensioning technologies have been studied during recent years in the OECD NEA/CSNI launched activity. Some of the findings are mentioned here. They have not yet been published, but the drafts regarding the topic of this paper have been prepared by OECD/Abrishami (2013) and OECD/Varpasuo (2013).

Design level

Comparison of grouted and greased tendons has shown that grouted tendons provide better corrosion protection, if the quality of the grouting is good. They provide a degree of bond between tendons and concrete. In order to ensure appropriate in-service inspections for post tensioned containment it is practical to have some greased tendons for direct monitoring even if the overall solution is grouted tendons. All greased tendons can be physically inspected if required. They can be re-tensioned and replaced if required, but in practice the work would be very difficult and even dangerous.

In the event of concrete cracking and if the tendons are grouted, the cables contribute as passive reinforcement to limit the cracks opening. The tension along the tendon is not uniform, but higher on the crack than between two cracks. Even if the rebar is yielding, the grouted tendons can contribute to limit the cracks opening. For unbonded tendons the tension is about uniform along the tendons and is limited by the average concrete strain.

Gallitre et al. (2012) summarized that greased cables have the main advantage of allowing direct in-service control of the force which is effectively in the cable end and the main drawback is that an active maintenance has to be done to survey the corrosion protection that can evolve during the lifetime of the plant. At the opposite, the grouted technology has to be very well managed during the construction phases in order to have corrosion protection, and then during the plant operation, reduced action is needed, such as global strain monitoring system for full pressure test survey and for pre-stress losses assessments. An important part for in-service inspections for both post-tensioning systems is supportive monitoring analyses.

Beyond design level

In the event of rupture of a grouted tendon, the cables contribute to re-anchor themselves and continue to act as passive reinforcement and resist some of the force previously resisted by the ruptured tendon. For greased tendons, when a rupture occurs the force that was resisted by the ruptured tendon must be taken up by the surrounding tendons.

The localization of the containment failure under over-pressure is different for unbonded tendons and for grouted tendons. The location of the main failure is close to the ribs in case of grouted tendons, because it is the point where the initial tendon tension is higher. The case is more uncertain for unbonded tendons, because of the redistribution of stress along the tendons.

Modelling greased tendons as ‘bonded’ elements, such as rebar layers or embedded truss elements, can produce approximate results but can lead to premature prediction of tendon rupture as tendon strain increase is equal to containment wall strains. Modelling grouted tendons as ‘bonded’ elements will produce realistic results for most studies. Great care must always be exercised in implementing the proper stress distribution along the tendons. As expected, the displacements of the bonded model vary more, but the maximum values stay lower.

Gallitre et al. (2012) summarized that in accidental conditions also, the local containment behavior may differ depending on the post-tensioning technology, due to the local bond forces between the cables and the concrete itself: the greased tendons can slip along the ducts when pressure increases which may lead to strain localization effects that could impact liner tightness at beyond design pressure level. For this last aspect, only advanced numerical calculations can investigate this concrete cracking phenomenon. The most challenging question for computations is the slipping of greased tendons.

It is worthwhile to refer to a draft which deals with beyond-design calculation, prepared within the activity by OECD/Varpasuo (2013). The internal pressure capacity in this estimation is an internal pressure at which the structural integrity is retained and a failure leading to a significant release of fission products does not occur. The failure of a PCCV is highly dependent on displacements. When the radial displacement of the centre part of the cylinder far from the discontinuities and local damages starts to increase, a sudden change in the global stiffness of the structure and thus the ultimate failure has been reached.

For cylindrical containment structures the use of analytical solution formulas to estimate the pressure capacity are possible as first link in the analysis sequence. The initial condition for the nonlinear analysis of the containment structure should be the linear elastic response caused by dead load and design pressure, at the design temperature. The internal pressure is incrementally increased until a failure is reached. The pressure capacity for cylindrical pre-stressed concrete containments is to be based on the contribution from each structural element considered in the analysis, using the stress-strain curve for each material and the strain level in each material, as determined based on overall strain compatibility between all of the credited structural elements such as concrete, liner, tendons and reinforcement bars. The ISP48 was analytically calculated as an example by Varpasuo and, according to that, the pressure and displacement of the cylinder wall are

- at liner yield: 0.95 MPa ($2.4 P_d$) and 5.38 mm
- at rebar yield: 1.17 MPa ($3.0 P_d$) and 10.76 mm
- at ultimate failure 1.57 MPa ($4.0 P_d$) and 32.3 mm

They are in good agreement with the test results.

In a study by Kähkönen et al (OECD NEA CAP, 2011), it was observed that the tendon stress distributions were different in bonded and unbonded cases, which led to lower ultimate failure capacity by approx. $0.3 P_d$ for the unbonded case. The FE model used in that study was nearly identical to the one described below in this paper. The main difference is that Kähkönen used connector elements (of type “slot”) for each node in truss elements, but no contact surfaces, to model the interaction between concrete and tendons. On the other hand, some preliminary studies by other benchmark participants came into an opposite conclusion.

SIMULATIONS

Finite Element Model

The FE mesh was provided by Fortum, see Vuorinen et al. (2010). It includes concrete structure as shell elements, main openings, reinforcement as smeared layers, tendons as truss elements and the steel liner as shell elements. The model takes into account post-tensioning with angular wobble and anchor slip losses, slippage between tendons and concrete and possible grouting of tendons. It also takes into account the concrete damage and failure of tendons and rebars. The non-linear dynamic FE analyses were conducted with Abaqus/Explicit version 6.12-1, see Dassault Systèmes (2012), using single core and double

precision. The PCCV test and FE models are shown in Figure 1. An approach was chosen where the main part of the interaction between the concrete and the tendons is realized by contact formulations while some so-called connector elements of type “slot” are needed as well (shown in red in the center figure). The slot connectors, shown in more detail in Figure 2, allow displacements only in one locally defined direction. Post-tensioning is achieved by defining forces and displacements to the connectors at tendon ends (see Figure 2, on the right). The contact surfaces lie initially 1 cm both inwards and outwards from the tendons in the axial direction of the containment wall.

Figure 3 shows the stress-strain relation used in FE analyses for different steels (left) and concrete (right). A von Mises plasticity model was used for all the steel materials. The “concrete damaged plasticity” model was used for concrete. The analysis time was 3 seconds. The mass of the whole model was multiplied by 100 in order to damp out vibration and increase the time step size. Partly for this reason, gravitational forces were not considered. The total number of elements in the model was 88 336.

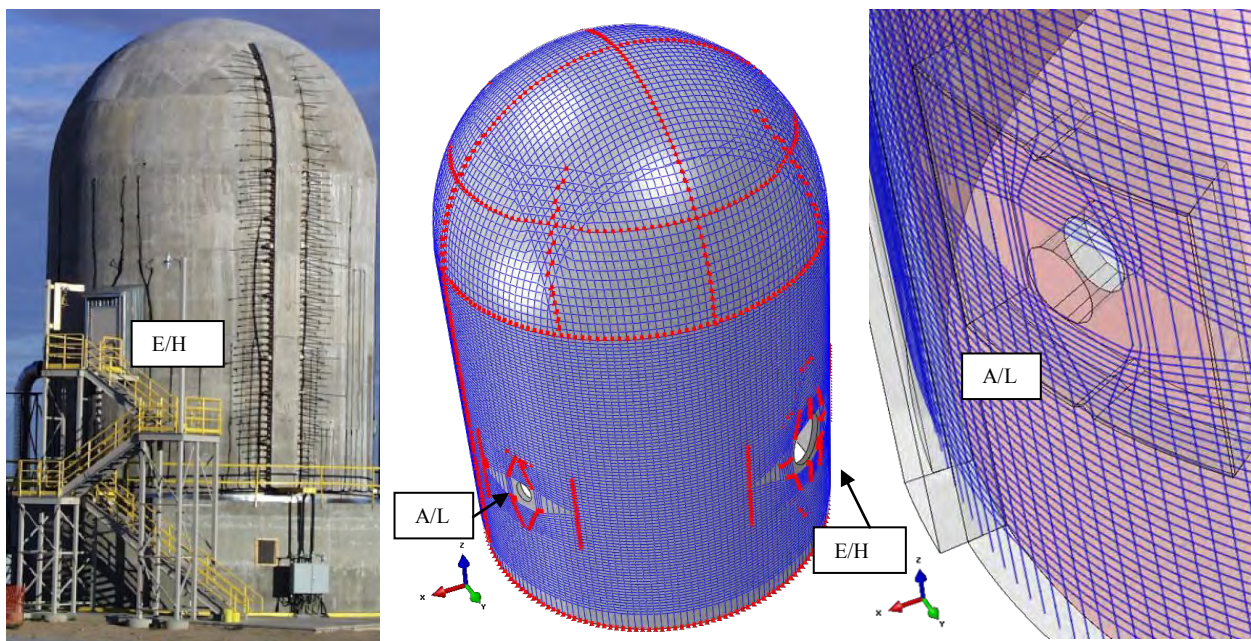


Figure 1. PCCV test model (left), FE model (centre) with connectors shown in red and detail of the FE model around A/L (right).

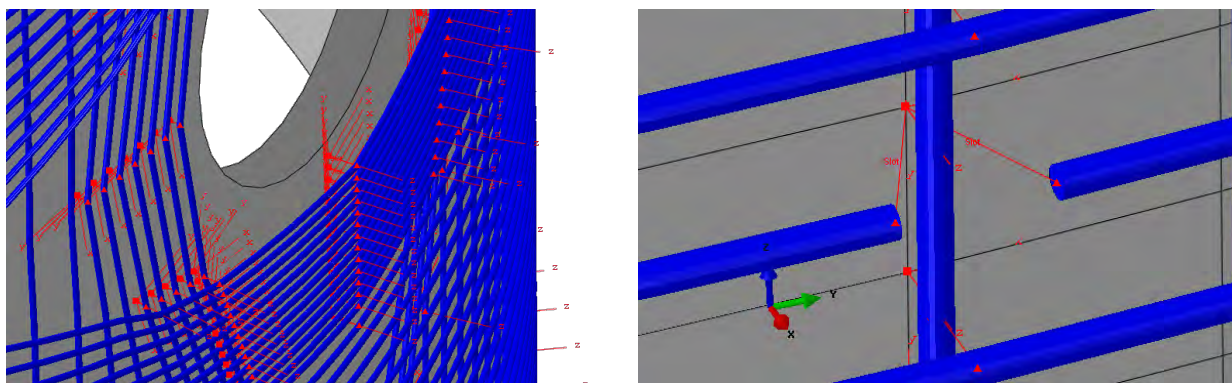


Figure 2. FE model details around E/H (left) and at the anchoring buttress (right) with connectors.

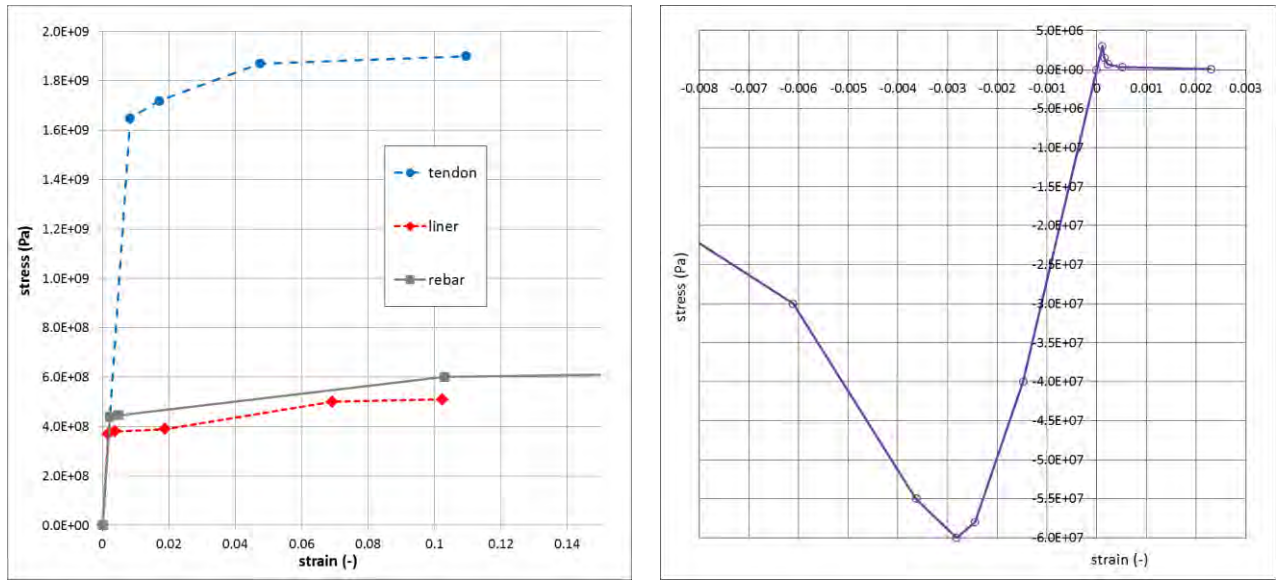


Figure 3. Stress-strain relation used in FE analyses for different steels (left) and concrete (right).

Main simulation cases and results

The simulations were conducted in four steps. Table 1 shows the main analysis cases and their conditions at different steps. Figure 4 shows the stress distribution in hoop tendon H70 after pulling the tendons and after seating, according to FE simulation and analytical calculation (left). Some experimentally measured values are also shown. Also, the stress distribution in H70 during SFMT in three cases at different overpressures during SFMT is shown on the right. Case “unbonded B” is an artificial case where the tendons were gradually loosened during the last step in order to achieve larger sliding and consequently redistribution of stresses. The ultimate failure pressure for corresponding “bonded B” was even lower, approx. $3.9 P_d$.

Table 1: Main analysis cases and steps.

Step	bonded	unbonded A	unbonded B
Initial state	material properties, initial and boundary conditions, connector behaviour definitions	as in bonded	as in bonded
Step 1 (pulling)	force in tendon end connectors	as in bonded	as in bonded
Step 2 (seating)	displacement in tendon end connectors	as in bonded	as in bonded
Step 3 (pressurising)	increase friction coefficient, “lock” all the connectors, pressure to liner (linearly ramped up from 0 bar to 30 bar)	as in bonded , but lock only tendon end connectors	as in unbonded A , but displacement in tendon end connectors (linearly to 5 cm)
Ultimate failure pressure	$4.5 P_d$	$4.5 P_d$	$4.1 P_d$

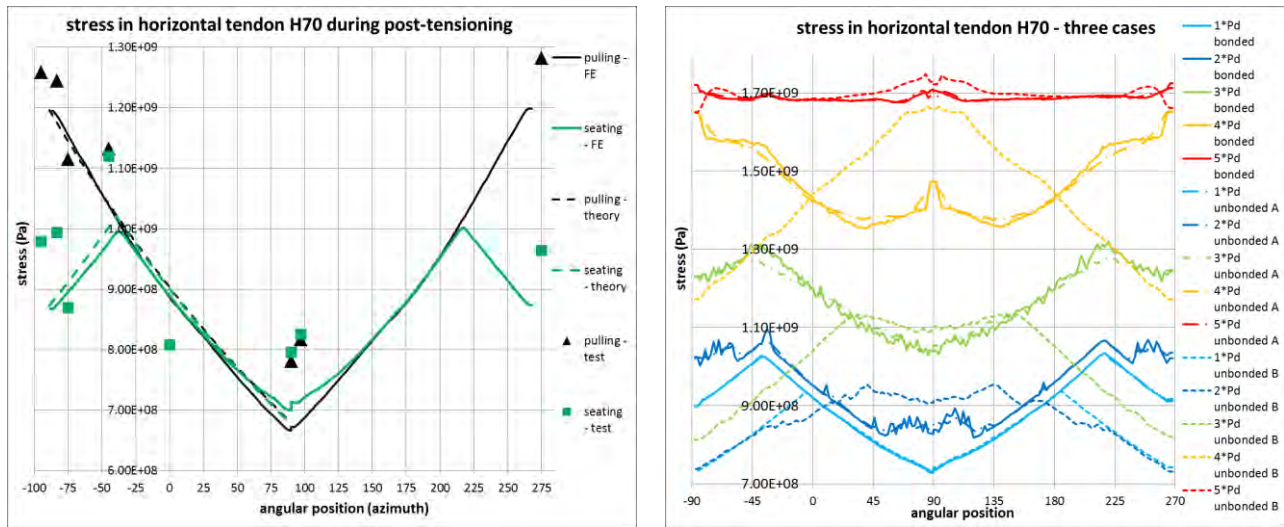


Figure 4. Stress distribution in horizontal tendon H70 after pulling the tendons and after seating, according to FE simulation and analytical calculation (left). Stress distribution in H70 during SFMT in three cases (right).

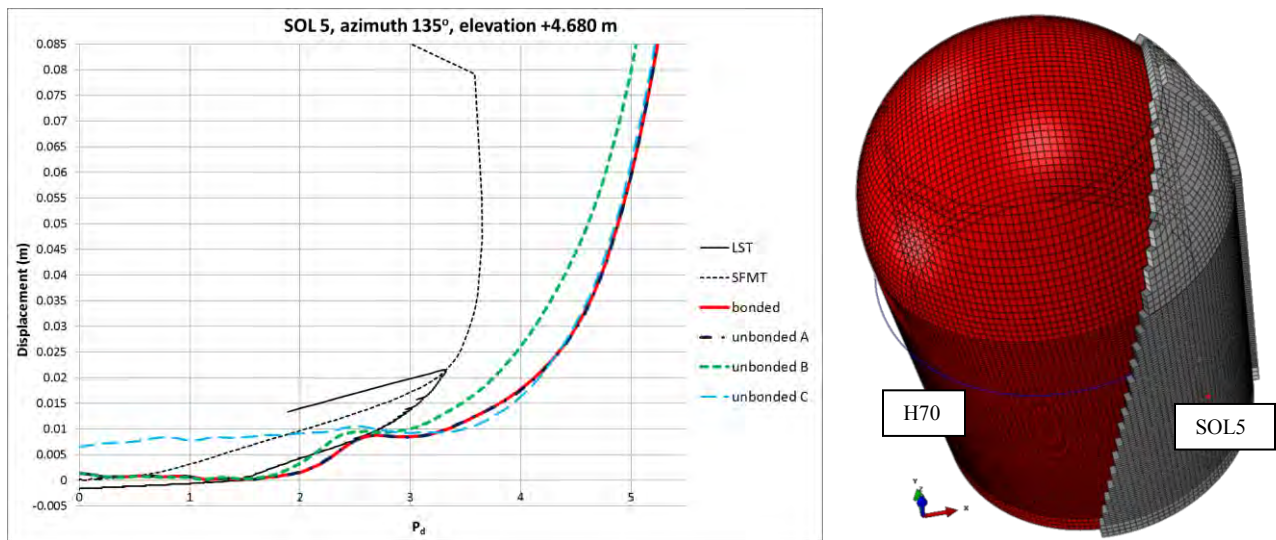


Figure 5. Radial displacement as function of pressure of SOL5 during LST, SFMT and simulation of SFMT in different cases (left). Locations of SOL5 and tendon H70.

Figure 5 shows radial displacement as function of pressure of standard output location SOL5 during LST, SFMT and simulation of SFMT in different cases (left). Locations of SOL5 (red dot) and hoop tendon H60 (blue line) are shown on the right. The liner is coloured in red. The simulation of LST test was included in Step 3 of case “unbonded C” shown in Figure 5.

Figure 6 shows displacement magnitude at $3.8 P_d$ (left) and plastic strain in tendons at $5.4 P_d$ in case “unbonded A” (right). The maximum displacement values are in the area where the test structure ruptured. The tendons ruptured in most simulations first between the A/L and anchor buttress as can be seen on the right.

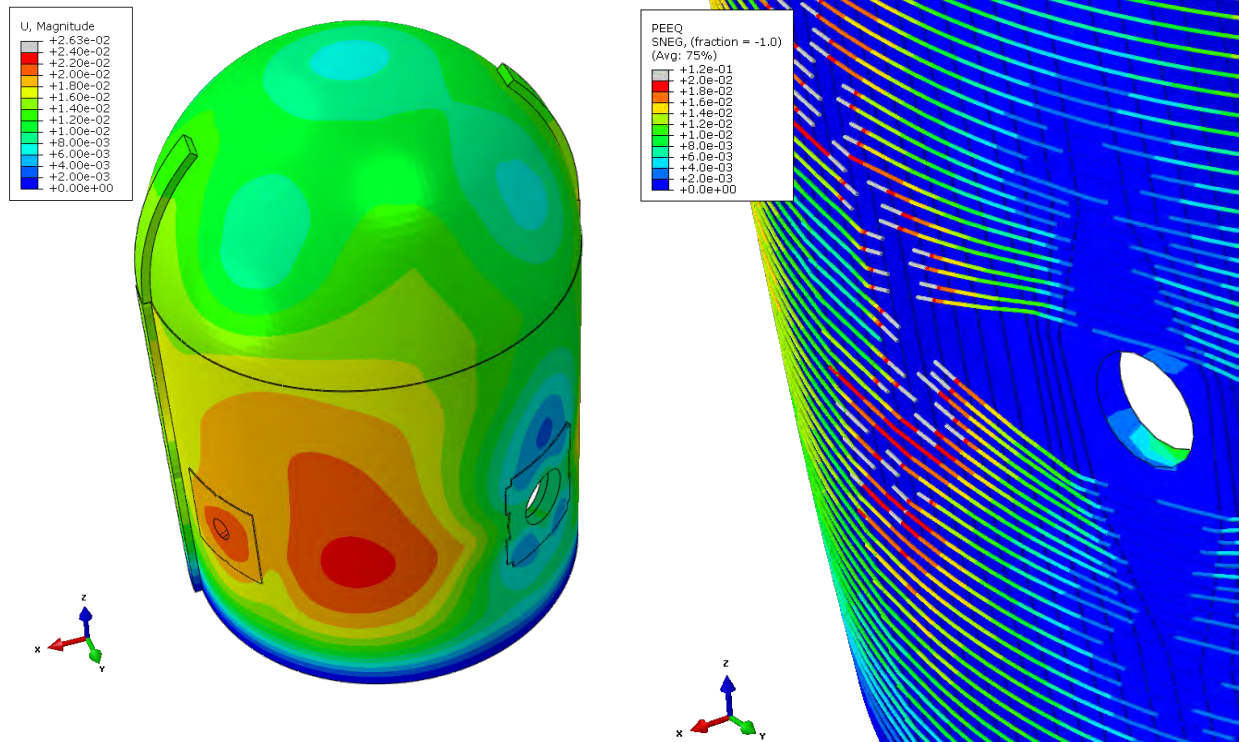


Figure 6. Displacement magnitude at $3.8 P_d$ (left) and plastic strain in tendons at $5.4 P_d$ in case “unbonded A”.

Sensitivity studies

In addition to the main cases considered above, some sensitivity studies were done by varying the friction coefficient in the tendon behavior and the tendon failure strain. When the friction is half of the original one, the ultimate failure capacity increases by $0.2 P_d$. When it is sixth of the original one, capacity increases by $0.3 P_d$. When the friction is doubled, the capacity decreases by $0.3 P_d$. Tendon failure strains of 1%, 2%, 4% and 5% were implemented. The model ruptures earlier with lower failure strains, but this effect takes place only after the structural stability has already been lost and thus does not affect the ultimate failure capacity. All these observations apply similarly to both bonded and unbonded models.

CONCLUSION

The over-pressurization tests of the 1:4 scale PCCV model represents a significant advance in understanding the capacity of nuclear power plant containments to loads associated with severe accidents. The data collected during the tests, as well as the response and failure modes exhibited, have been used for many years and will be used for many years to come to benchmark numerical simulation methods used to predict the response of concrete containment structures. The PCCV model tests have demonstrated the importance of the unique details and as-built characteristics of the model on the ultimate capacity. Any efforts to estimate the capacity of an actual containment must address the unique features of the plant under consideration.

The FE model was capable of predicting the behaviour of the PCCV during the post-tensioning phase as well as in case of increasing overpressure up to the point of rupture. The results indicate that one

of the most critical locations is where the rupture initiated in reality and that the ultimate failure capacities for both cases, with grouted or greased tendons, are close to each other.

The force distribution in the tendons before the overpressurization was able to be modelled in a correct manner by simulating the pulling of tendons, anchor seating and locking. The simulated distribution was verified against simplified analytical calculation and some experimental measurements. The FE model overestimated by approx. 10-20% ($3.6 P_d$ compared to $4 - 5 P_d$) which could be anticipated. It is difficult to deduce from the simulation results the exact point of failure. FE models usually have a higher capacity, since they do not have imperfections in the same sense than real structures (unless they are intentionally added). Furthermore, if several tendons break in certain location, it easily leads to a breach through the wall whereas the FE model in this study is not able to directly simulate breaching but allows increase of pressure until the analysis terminates due to numerical instabilities. In any case, the first tendon breaks in test were observed at $3.4 P_d$ whereas in simulation the first tendons broke at approx. $5 P_d$ when 5% failure strain was used. The test model ruptured finally between the two main penetrations whereas for the FE model it is more difficult to designate any single location. Some results, such as the radial displacement peaks, i.e. local bulging of the PCCV, indicate the same location.

The model displacement results show an interesting plateau between approx. $2.5 P_d$ and $3.5 P_d$ (depending on the location) where the displacements do not increase with increasing pressure. This is seen also in the some energy components. It appears as if the structure is behaving like an elastic string during that phase, gathering internal energy, until it finally gives in to the pressure. This may explain the difference of same magnitude in the ultimate capacities. For some reason, the FE model has elastic capacity for approx. $1 P_d$ more than the real one. It is possible that effect of basemat and pre-cracking of real structure has a stronger effect than considered in analyses.

The analyses in this study did not show any major differences between the results with bonded and unbonded methodologies. The ultimate capacity for unbonded case is only very slightly lower than for the bonded case. However, it seems that the model is not capable of simulating the tendon slipping and thus the redistribution of tendon stresses efficiently enough during overpressurization. One reason for this is the relatively small number of connector elements which leads to sharp turns which seem to lock the tendons to some degree. Furthermore, this model was not able to create an ideal perfect bond throughout the whole length of the tendon in bonded case. On the other hand, there may not be that much difference in this respect between these cases as has been commonly believed.

It is a rather surprising conclusion that the application of failure criterion for tendons does not considerably seem to affect the results. The tendons rupture only after the structure has already failed. Furthermore, changing the failure criterion from 5% to 1% equivalent plastic strain did not decrease the ultimate capacity of the structure. The rupture was only somewhat faster. It has been inferred that the tendon strains on average in the test were approximately 2% when the first tendons ruptured. Almost half of this is elastic.

The “concrete damaged plasticity” material model works well in this type of analysis. The concrete was damaged extensively after $2 P_d$. Also, more moderate damage parameter values were used, in which case the ultimate capacity increased slightly but generally there was not any substantial change in the behaviour of the structure.

A modelling procedure that creates reliable models that can be applied for different types of PCCVs has now been developed. The most important and at the same time the most difficult task remains the same: to model the interaction between tendons and concrete. An approach was chosen where the main part of the interaction is realized by contact formulations, but some connector elements are still needed as well. Thus, it is not the most elegant way. It demands a lot of time for modelling.

One option to model the interaction even more accurately is to explicitly model the ducts within which the tendon elements go. The ducts, which are most conveniently modelled with shell elements, are then tied to concrete elements. Contact interaction is defined between the tendons and ducts. Another option, more practical one in the long run, could be to create a new user-defined element for keeping the tendons in their path and enabling bonds of different degrees during the analysis.

It is commonly believed that unbonded post tensioning system is more susceptible to get global sudden rupture than bonded system with a residual load carrying capacity after local ruptures. This study does not clearly support that thinking. The first leaks initiate before rupture. The tendons start to break one by one, even though relatively fast. The study shows that regarding the ultimate capacity, the post-tensioning is more important than the grade of bonding after it, and the amount of reinforcement and tendon cables are determinant.

Future studies will show more benefits and drawbacks of this type of procedure compared to others. Unfortunately, no common conclusions on a detailed level have yet been drawn within the OECD benchmark regarding the effect of bonding on the ultimate capacity. Preliminary comparison shows that the benchmark participants use mainly similar modelling approaches. All are able to simulate the realistic tendon stress distribution. The other studies predict the ultimate capacity and the displacements slightly more accurately than the one presented here. One reason for this might be the fact, that only this study did not include the basemat. A completely 3D model with solid elements for the concrete would be able to give locally more accurate results, but would require substantially more effort. There are discrepancies in the evaluation of the two post-tensioning methodologies. This second goal of the benchmark study still remains as a challenging study.

REFERENCES

- Abaqus Theory Manual, version 6.12-1. Dassault Systèmes, 2012.
- Gallitre, E., Varpasuo, P., Huerta, A., Valfort, J-L. "POST-TENSIONING METHODOLOGIES FOR CONTAINMENT BUILDING: GREASED OR CEMENT GROUTED TENDONS – CONSEQUENCES ON MONITORING, PERIODIC TESTING AND MODELLING ACTIVITIES". NUCPERF 2012, 12 - 15 November 2012, Cadarache, France.
- NUREG/CR-6810, SAND2003-0840P, Project Report No. R-SN-P-010. "Overpressurization Test of a 1:4-Scale Prestressed Concrete Containment Vessel Model", 2003. Prepared by M. F. Hessheimer, E. W. Klamerus, L. D. Lambert, G. S. Rightley, Sandia National Laboratories.
- NUREG/CR-6809, SAND2003-0839P, ANA-01-0330. "Post-test Analysis of the NUPEC/NRC 1:4 Scale Prestressed Concrete Containment Vessel Model", 2003. Prepared R.A. Dameron, B.E. Hansen, D.R. Parker, Y.R. Rashid.
- OECD NEA CAP meeting, 2011 April 20 - 22, Lyon, France.
- OECD NEA/CSNI launched activity "OECD Post Tensioning Methodologies for Containment Building: Greased or Cement Grouted Tendons - Consequences on Monitoring, Periodic Testing and Modelling Activities". Report Draft, Chapter 4.1, Design level, prepared by Abrishami (reviewed by H., Barré, F.) and Chapter 4.2, Beyond design level, prepared by Varpasuo, P., 2013.
- Vuorinen, M., Kähkönen, J., Varpasuo, P. "PCCV SPE3 MODEL 1 SIMULATION: FORTUM LTD", Fortum Power and Heat Ltd, 2010.